Conformational Changes in G-CSF/Receptor Complex As Investigated by Isotope-Edited FTIR Spectroscopy

Tiansheng Li,* Tom Horan, Tim Osslund, George Stearns, and Tsutomu Arakawa

Protein Chemistry Department, M/S 14-2-D, Amgen Incorporated, 1840 Dehavilland Drive, Thousand Oaks, California 91320

Received October 29, 1996; Revised Manuscript Received May 20, 1997[⊗]

ABSTRACT: Conformations of G-CSF and the extracellular domain of its receptor as well as their complex have been investigated by employing isotope-edited FTIR spectroscopy. To determine unambiguously the protein conformations of G-CSF and the receptor in the complex, we have prepared uniformly $^{13}C/^{15}N$ isotope labeled G-CSF to resolve its amide I′ band from that of the receptor in the IR spectrum of the complex. By comparing the IR spectra of the isotope-labeled G-CSF and the receptor with that of the complex, we have provided spectral evidence that the AB loop region involving the unique 3_{10} helix segment of G-CSF likely undergoes a conformational change to a regular α-helix upon binding to the receptor. The IR data also indicate a possible minor increase in α-helical conformation for the receptor in the complex. Furthermore, FTIR spectra of G-CSF, the receptor, and their complex demonstrate clearly that protein conformations of both G-CSF and the receptor have been dramatically stabilized by complex formation. Specifically, the melting transition (T_m value) of the α-helix in G-CSF is increased by nearly 30 °C and that of the β-strand in the receptor by nearly 15 °C in the G-CSF/receptor complex. We estimate from the current FTIR data that the native conformations of approximately 15% of all receptor residues are stabilized by G-CSF binding. On the other hand, the entire α-helical content of G-CSF appears to be stabilized in the complex. Together, these results indicate that formation of the ligand/receptor complex results in not only conformational changes in the receptor but also significant structural changes in the ligand. This adds insight to the general consensus that binding of ligand to cytokine receptors induces mostly structural changes in the receptor which lead to receptor oligomerization and signal transduction. The current data also suggest a possible physiological role of the 3_{10} helix present in G-CSF for its receptor binding activity.

G-CSF is one of the colony-stimulating factors (CSF) which stimulate granulocyte formation from bone marrow cells upon binding to its receptor (Nicola et al., 1983; Souza et al., 1986; Clark & Kamen, 1987; Nagata & Fukunaga, 1991). Although it is believed that ligand-induced receptor oligomerization results in eventual signal transduction, involvement of conformational changes of the receptor in oligomerization or signal transduction has also been suggested (Stahl & Yancopoulos, 1993; Heldin, 1995). The crystal structure of G-CSF (Hill et al., 1993) shows that it shares main structural features, i.e., four α-helix-bundles with up−up−down−down connections, with other cytokines such as growth hormone (GH) (Abdel-Meguid et al., 1987; de Vos et al., 1992), IL-2 (Bazan, 1992; McKay, 1992; Mott et al., 1992), IL-4 (Smith et al., 1992; Powers et al., 1992; Wlodawer et al., 1992), and macrophage colony-stimulating factors (M-CSF and GM-CSF) (Diederichs et al., 1991; Walter et al., 1992; Pandit et al., 1992). Aside from sharing the main structural features with other cytokines, the crystal structure of G-CSF reveals a unique 3_{10} helix segment in the long AB loop just after helix A (Hill et al., 1993). However, it remains unclear what role this 3_{10} helix segment of G-CSF may play in the process of receptor binding. Recent biophysical studies suggest that G-CSF forms a 2:2 complex with the soluble form of the receptor prepared from Chinese hamster ovary cells (Horan et al., 1996). In the absence of G-CSF, the receptor weakly dimerizes. Upon binding of G-CSF, however, the affinity of receptor dimerization is drastically increased by 2000-fold, suggesting conformational changes in the complex. Since the three-dimensional structure of neither G-CSF receptor nor receptor/ligand complex is available, the structural aspects of G-CSF/receptor interactions remain to be fully characterized. Structural determination of the extracellular domain of the G-CSF receptor by X-ray and NMR so far has been a challenge because of glycosylation and the molecular size of this receptor. FTIR spectroscopy has been proven to be an effective tool to study secondary structures of proteins in various physical states (Byler & Susi, 1986, 1988; Arrondo et al., 1993; Jackson & Mantsch, 1995; Haris & Chapman, 1995). Haris and co-workers have first demonstrated that by ^{13}C uniform labeling of amide C═O groups the amide I′ band of a protein can be shifted to ∼40−45 cm^{-1} lower in frequency, and that it is thus possible to determine secondary structures of individual subunits in a protein/protein or protein/peptide complex (Haris et al., 1992). This method has recently been applied to other protein/protein and protein/peptide systems (Zhang et al., 1994; Ludlam et al., 1995). Since ^{13}C═O groups shift amide I′ bands to approximately 40 cm^{-1} lower in frequency relative to those of ^{12}C═O amide groups (Hubner et al., 1990; Tadesse et al., 1991; Haris et al., 1992; Martinez et al., 1994), it is possible to resolve the amide I′ bands of two protein subunits in a protein/protein complex. Here, we have applied this technique for the first

* To whom correspondence should be addressed. Telephone: 805-447-8502. Fax: 805-499-6474. E-mail: li@amgen.com.

[⊗] Abstract published in *Advance ACS Abstracts,* July 1, 1997.

S0006-2960(96)02713-4 CCC: $14.00

time to the structural study of cytokine−receptor interactions and demonstrated its usefulness in determining unambiguously the protein secondary structures of both ligand and receptor in a signal transduction complex. We have investigated the structural changes in G-CSF and its receptor upon complex formation, and have shown that both G-CSF and the receptor likely undergo conformational changes in the complex.

MATERIALS AND METHODS

Purifications of $^{13}C/^{15}N$-Labeled G-CSF and Receptor/G-CSF Complex. An *Escherichia coli* K12 strain possessing a temperature-sensitive plasmid containing a gene coding for recombinant human G-CSF with the cysteine residue at position 18 replaced by an alanine was used. The strain was inoculated into 0.3 L of medium containing 20 g/L $(^{15}NH_4)_2SO_4$, 2 g/L K_2HPO_4, 2.4 g/L KH_2PO_4, 10 g/L [$^{13}C_6$]glucose, 1.2 g/L $MgSO_4 \cdot 7H_2O$, and 1 mL/L vitamins and trace metals (Curless et al., 1991) and grown 24 h with shaking at 30 °C. The entire culture was transferred to a 2-L sterile vessel (B. Braun) containing 1.5 L of minimal medium that contained 30 g/L $(^{15}NH_4)_2SO_4$, 2.7 g/L sodium hexametaphosphate (Curless et al., 1996), 0.4 g/L KCl, 13.3 g/L [$^{13}C_6$]-glucose, 2 g/L $MgSO_4 \cdot 7H_2O$, and 1 mL/L vitamins and trace metals. This batch phase of the fermentation was performed at 30 °C with neutralization by phosphoric acid and sodium hydroxide. Upon exhaustion of the glucose, concentrated feed containing 90 g/L [$^{13}C_6$]glucose, 27 g/L $(^{15}NH_4)_2SO_4$, 1.0 g/L $MgSO_4 \cdot 7H_2O$, and 1 mL/L vitamins and trace metals was fed into the vessel at the rate of 0.5 (mL/L)$\cdot OD^{-1} \cdot h^{-1}$. When the culture had reached an optical density of 15 at 600 nm, the culture was induced by increasing the temperature to 40 °C, and the feed was replaced with another containing 80 g/L $(^{15}NH_4)_2SO_4$, 90 g/L [$^{13}C_6$]glucose, 1.0 g/L $MgSO_4 \cdot 7H_2O$, and 1 mL/L vitamins and trace metals. The second feed was added to the fermentor at a rate of 25 (mL/L)$\cdot h^{-1}$. After 5 h of induction, the entire volume of the vessel was harvested by centrifugation. Purification of $^{13}C/^{15}N$-labeled G-CSF follows essentially the same procedure as that of natural G-CSF (Souza et al., 1986).

Affinity-purified soluble G-CSF receptor containing the entire extracellular domain (from CHO cell conditioned media) was mixed with a 2-fold molar excess of either natural or isotope-labeled G-CSF for 1 h at 4 °C. The mixture was injected onto a Superdex-200 (HR 26/60) column connected to an FPLC system (Pharmacia). The column was equilibrated with 0.1 M potassium phosphate, pH 6.7, and run at a flow rate of 1.0 mL/min, monitoring the eluent at A_{280nm} and collecting 2.5 min fractions. Peak fractions (from 46 to 50) corresponding to complex were pooled and then concentrated and buffer-exchanged using a Centricon-30 ultrafiltration device (Amicon).

FTIR Spectroscopy. Stock solutions of G-CSF in NaOAc, pH 4.5, buffer were concentrated and hydrogen−deuterium-exchanged into 10 mM sodium phosphate, 50 mM NaCl, pD 7.0, buffer using a Centricon (Amicon) cartridge with a membrane of 10 kDa molecular mass cutoff. Diafiltration of G-CSF in D_2O buffer was repeated several times to ensure complete H−D exchange. The final protein concentrations were approximately 10 mg/mL before IR data collection, and the protein solution was injected into a sample holder consisting of a pair of CaF_2 windows with a 25 μm spacer to form an uniformly thin film. Sample temperature was maintained at 20 °C during IR data collection using a thermal jacket controlled by an electronic thermal controller (Boulder Nonlinear Inc.). Typically, 1024 interferograms were co-added and Fourier-transformed to generate an absorbance spectrum at 4 cm^{-1} resolution by employing a Mattson Research Series Model 1000 spectrometer with a MCT detector cooled by liquid nitrogen. The spectrometer was continuously purged with a dry air system (Model 75-60, Balston Filter System, Whatman) to eliminate the spectral interference from atmospheric water vapor. Residual contributions from atmospheric vapor were digitally subtracted from the protein spectra. The broad buffer background of D_2O was subtracted from protein spectra to ensure a flat base line in the spectral region 1400−1800 cm^{-1}. IR spectral analysis, including spectral deconvolution and calculation of second-derivative spectra, has been carried out by employing Grams/386 and Spectral Calc softwares (Galactic Industries Co.).

RESULTS

The binding activities of both unlabeled and $^{13}C/^{15}N$ uniformly labeled G-CSF were compared (Figure 1) using the entire extracellular domain of human G-CSF receptor purified from Chinese hamster ovary cells (Horan et al., 1996). As shown in Figure 1, biological activities of the two different isotopic G-CSF proteins are virtually identical in terms of receptor binding. The two complexes eluted at identical volumes from a size exclusion column (Figure 1A, top and bottom panels) and migrate at the same positions on the native gel (data not shown). Peak fractions corresponding to both isotope-labeled and unlabeled G-CSF/receptor complexes were confirmed by reducing SDS−gel electrophoresis, as shown in Figure 1B (top and bottom panels). The receptor and G-CSF migrated at 97 and 18 kDa, respectively. The purified G-CSF/receptor complexes from the size exclusion column were used for the following FTIR studies.

The FTIR spectrum of $^{13}C/^{15}N$ uniformly labeled G-CSF is compared to that of the unlabeled protein, as shown in Figure 2 (A, left, and B, right). Both original and deconvolved spectra in the region 1400−1750 cm^{-1} (Figure 2A, left panel) of the labeled G-CSF indicate that isotope labeling of the amide groups of G-CSF is fairly complete, since the spectrum of the labeled G-CSF (Figure 2, left panel, spectra C and D) shows minimal IR intensity and is close to base line near 1653 cm^{-1} where the unlabeled G-CSF gives rise to peak IR absorbance (Figure 2A, left panel, spectra A and B). In addition, the amide II′ band at 1455 cm^{-1} of the unlabeled G-CSF is shifted to 1405 cm^{-1} for the labeled protein. The weak amide II bands centered at 1566 cm^{-1} for the unlabeled G-CSF and at 1525 cm^{-1} for the labeled protein indicate that most amide NH groups of the free G-CSF undergo H−D exchange. Figure 2B (right panel) compares the second-derivative FTIR spectra of the two isotopic forms of G-CSF in the amide I′ region 1700−1550 cm^{-1}. It is clear that the spectra of isotope-labeled and unlabeled G-CSF have identical spectral features except for frequency shift.

Figure 3 shows the FTIR spectra including the original (Figure 3A, left panel) and deconvolved (Figure 3B, right panel) spectra in the region 1400−1800 cm^{-1} of ligand-free

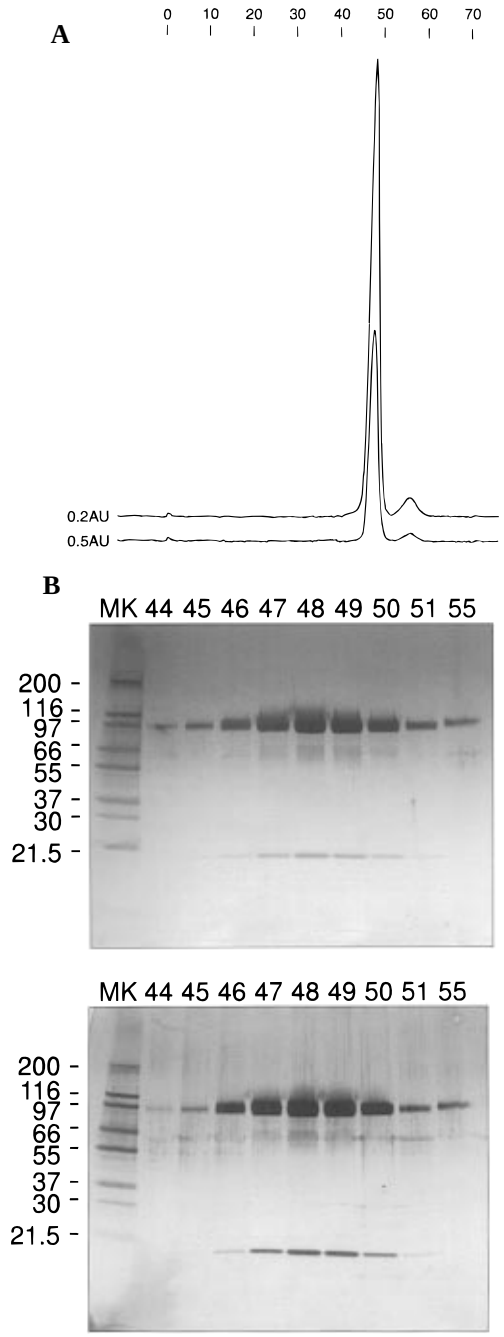

FIGURE 1: Comparison of the natural G-CSF/receptor complex with the $^{13}C/^{15}N$-labeled G-CSF/receptor complex. (A) Elution profiles of the two complexes from a Superdex-200 column (HR 26/60) (Pharmacia): top trace, $^{13}C/^{15}N$-labeled G-CSF/receptor complex; bottom trace, unlabeled G-CSF/receptor complex. (B) SDS gel of the two complexes under reducing conditions: top panel, fractions of $^{13}C/^{15}N$-labeled G-CSF/receptor complex from a Superdex-200 column; bottom panel, fractions of unlabeled G-CSF/receptor complex from a Superdex-200 column.

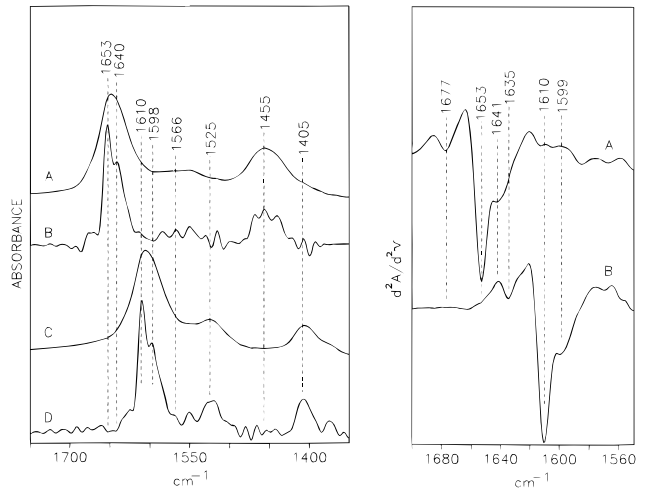

FIGURE 2: (A, left) Original and deconvolved FTIR spectra in the region 1350−1750 cm^{-1} of G-CSF in D_2O, 10 mM sodium phosphate, and 50 mM NaCl, pD 7.0. Spectrum A, original spectrum of the unlabeled G-CSF; spectrum B, deconvolved spectrum of the unlabeled G-CSF; spectrum C, original spectrum of the labeled G-CSF; spectrum D, deconvolved spectrum of the labeled G-CSF. (B, right) Second-derivative FTIR spectra in the amide I′ region 1550−1700 cm^{-1} of G-CSF protein. Spectrum A, unlabeled G-CSF; spectrum B, $^{13}C/^{15}N$ uniformly labeled G-CSF. The spectral deconvolutions were computed by using Spec Calc software (Galactic Industries Co.) and by choosing parameters γ 5.0 and filter 0.25.

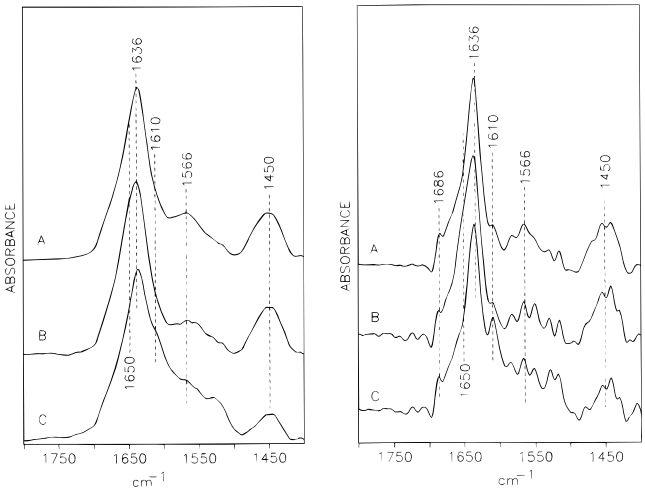

FIGURE 3: (A, left) Original FTIR spectra in the region 1400−1800 cm^{-1} of the free receptor (spectrum A), the unlabeled G-CSF/receptor complex (spectrum B), and the labeled G-CSF/receptor complex (spectrum C). (B, right) Deconvolved FTIR spectra in the region 1400−1800 cm^{-1} of the free receptor (spectrum A), the unlabeled G-CSF/receptor complex (spectrum B), and the labeled G-CSF/receptor complex (spectrum C). All proteins are dissolved into D_2O buffer containing 10 mM sodium phosphate and 150 mM NaCl, pD 7.0. The same parameters have been chosen for spectral deconvolutions as in Figure 2.

receptor, unlabeled G-CSF/receptor complex, and $^{13}C/^{15}N$ uniformly labeled G-CSF/receptor complex. Figure 4 shows the second-derivative FTIR spectra of the free receptor, unlabeled G-CSF/receptor complex, and labeled G-CSF/receptor complex. For unlabeled G-CSF, the peak frequency of its amide I′ band near 1650 cm^{-1} is separated by 14 cm^{-1} from that of the amide I′ band at 1636 cm^{-1} of the receptor (Figure 3A, spectrum B). The overlap of the two amide I′ bands of the receptor and the unlabeld G-CSF cannot be effectively resolved even by resolution enhancement through spectral deconvolution (Figure 3B, spectrum B) or the second-derivative spectrum (Figure 4, spectrum B). For the $^{13}C/^{15}N$ unifromly labeled G-CSF, however, the peak frequency of its amide I′ band at 1610 cm^{-1} is separated by 26 cm^{-1} from that of the receptor (Figure 3A, spectrum C). Consequently, the two overlapping bands of the labeled G-CSF and the receptor are well resolved by spectral deconvolution (Figure 3B, spectrum C). This is also demonstrated by the second-derivative spectra of the unlabeled G-CSF/receptor and the labeled G-CSF/receptor com-

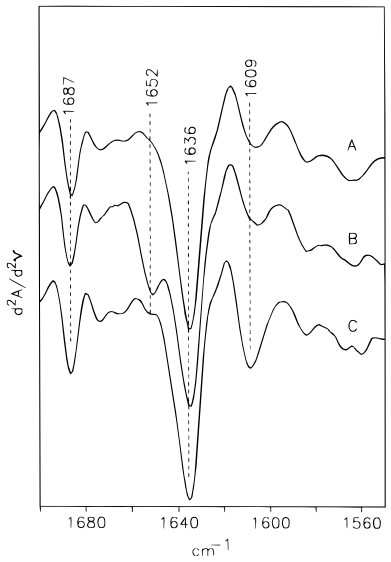

FIGURE 4: Second-derivative FTIR spectra in the amide I′ region 1550−1700 cm^{-1} of the free receptor (spectrum A), the unlabeled G-CSF/receptor complex (spectrum B), and the labeled G-CSF/receptor complex (spectrum C). Other conditions are the same as in Figure 2.

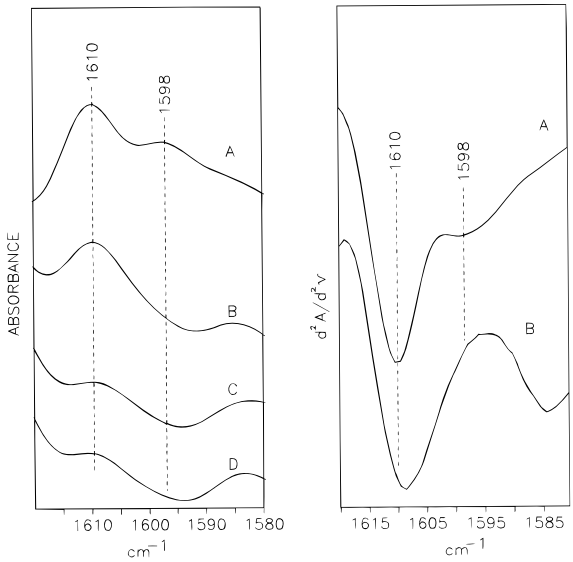

FIGURE 5: Comparison of the amide I′ band of $^{13}C/^{15}N$ uniformly labeled G-CSF in the free form with that of the labeled G-CSF in the complex. (A, left) Deconvolved FTIR spectra in the region 1580−1620 cm^{-1} of the labeled G-CSF in the free form (spectrum A), the labeled G-CSF in complex (spectrum B), ligand-free receptor (spectrum C), and unlabeled G-CSF/receptor complex (spectrum D). (B, right) Second-derivative IR spectra of the labeled G-CSF in free form (spectrum A) and the labeled G-CSF in the complex (spectrum B).

plexes, as shown in Figure 4 (spectra B and C). For the unlabeled G-CSF/receptor complex, the amide I′ band of G-CSF appears as a shoulder component at 1652 cm^{-1} next to the receptor band at 1636 cm^{-1} in the second derivative IR spectrum (Figure 4, spectrum B). For the labeled G-CSF/receptor complex, the amide I′ band at 1610 cm^{-1} of the labeled G-CSF is completely separated from that of the receptor band at 1636 cm^{-1} (Figure 4, spectrum C). It is noted that tyrosine residues of the receptor generate a weak IR band at 1610 cm^{-1}, which is overlapped with the amide I′ band of the labeled G-CSF in the complex. The peak intensity ratios of the 1610 cm^{-1} band over those of the

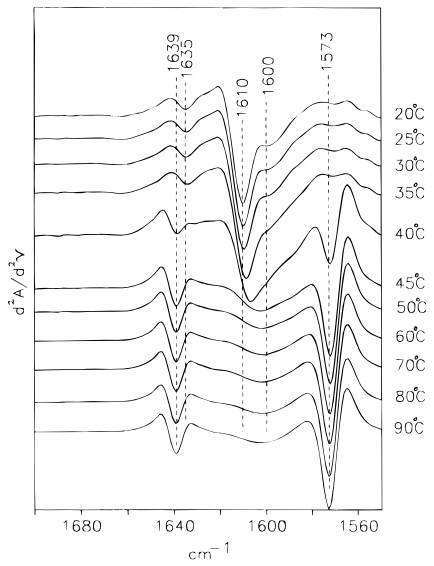

FIGURE 6: Second-derivative FTIR spectra in the amide I′ region of $^{13}C/^{15}N$ uniformly labeled G-CSF protein at temperatures from 20 to 90 °C (top to bottom spectra), in D_2O buffer containing 10 mM sodium phosphate and 50 mM NaCl, pD 7.0.

receptor band at 1636 cm^{-1} have been determined for the ligand-free receptor and the labeled G-CSF/receptor complex, to assess the extent of overlapping of these two bands. For the ligand-free receptor, the peak intensity ratio I_{1610}/I_{1636} is close to 0.24 (Figure 3B, spectrum A). This intensity ratio is increased to 0.52 for the labeled G-CSF/receptor complex, which reflects the intensity contribution from the amide I′ band at 1610 cm^{-1} of the labeled G-CSF (Figure 3B, spectrum C). To further examine if the overlapping of those two bands affects the shoulder component near 1600 cm^{-1} of the amide I′ band of the labeled G-CSF in the complex, we performed a detailed spectral comparsion of the labeled G-CSF in free and complex forms. Figure 5 compares the deconvolved (Figure 5A, left panel) and second-derivative (Figure 5B, right panel) spectra in the region 1580−1620 cm^{-1} of free G-CSF with those of the receptor-bound G-CSF. It is clear that the spectral contribution from the receptor is minimal at 1598 cm^{-1} though tyrosine residues of the receptor generate an IR band centered at 1610 cm^{-1} (Figure 5A, spectra C and D). It is therefore unlikely that for the complex the disappearance of the shoulder component of the amide I′ band at 1598 cm^{-1} of the labeled G-CSF results from the receptor band at 1610 cm^{-1}. A more likely explanation would be due to the conformational change in the labeled G-CSF in the complex, which leads to the disappearance of the amide I′ band at 1598 cm^{-1}. The possible conformational changes in G-CSF shall be examined further under Discussion.

To determine how complex formation of G-CSF with its receptor may affect the structural integrities of G-CSF and the receptor, we have carried out temperature studies of G-CSF, the receptor, and their complex. Figure 6 shows the second-derivative FTIR spectra of the labeled G-CSF alone in the temperature range 20−90 °C. Thermal transition of α-helix to β-sheet in G-CSF appears to start at around 40 °C, as evidenced by the appearance of the IR band at 1573 cm^{-1} and the decrease in IR intensity at 1610 cm^{-1}. In addition, there is a significant band broadening in the spectral region 1580−1610 cm^{-1} at 40 °C, suggesting the presence of a significant amount of irregular structures during the

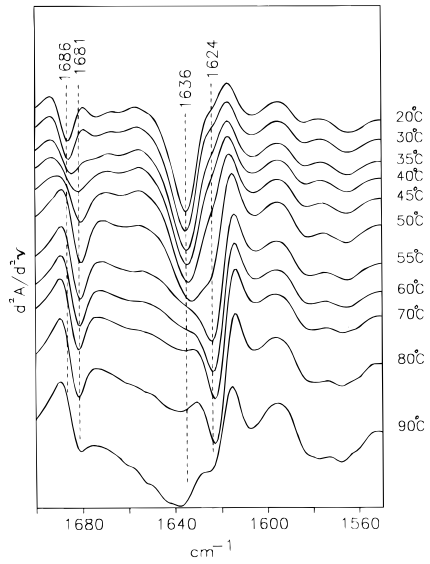

FIGURE 7: Second-derivative FTIR spectra in the amide I′ region of the extracellular domain of G-CSF receptor protein at temperatures from 20 to 90 °C (top to bottom spectra), in D_2O buffer containing 10 mM sodium phosphate and 50 mM NaCl, pD 7.0.

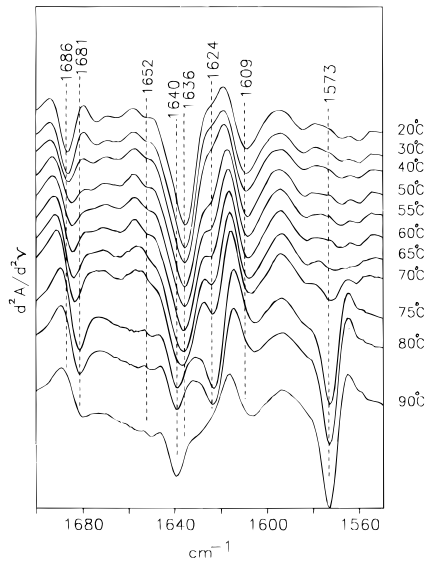

FIGURE 8: Second-derivative FTIR spectra in the amide I′ region of $^{13}C/^{15}N$-labeled G-CSF/receptor complex at temperatures from 20 to 90 °C (top to bottom spectra), in D_2O buffer containing 10 mM sodium phosphate and 50 mM NaCl, pD 7.0.

thermal transition of G-CSF. Figure 7 shows the second-derivative FTIR spectra of the free receptor in the temperature range 20−90 °C. The ligand-free receptor undergoes thermal transition starting at approximately 50 °C, with the conversion of native β-strands to intermolecular β-sheet, as indicated by the frequency shift of the 1636 cm^{-1} band to 1624 cm^{-1} and that of the 1686 cm^{-1} band to 1681 cm^{-1}. Figure 8 shows the second-derivative FTIR spectra of the labeled G-CSF/reeptor complex in the temperature range 20−90 °C. Thermal denaturations of the labeled G-CSF and the receptor in the complex can be followed by the intensity increases in IR bands at 1573 and 1624 cm^{-1}, respectively. Figure 9 compares the deconvolved FTIR spectrum of the ligand-free receptor with that of the labeled G-CSF/receptor complex at 55 °C, to estimate the amount of receptor residues stabilized by complex formation.

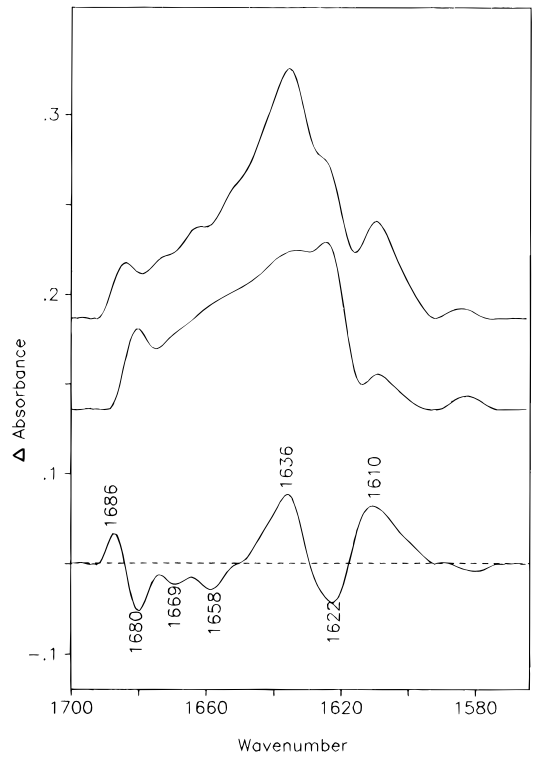

FIGURE 9: Deconvolved FTIR spectra in the amide I′ region of $^{13}C/^{15}N$-labeled G-CSF/receptor complex (top spectrum) and the free receptor (middle spectrum) at 55 °C. The difference spectrum (bottom spectrum) was computed by subtracting the spectrum of the free receptor from that of the complex (see also Results and Discussion). The spectral deconvolutions were computed by using Spec Calc software (Galactic Industries Co.) and by choosing parameters γ 5.0 and filter 0.25.

DISCUSSION

Solution Conformation of G-CSF. The peak of the amide I′ band shifts from 1653 cm^{-1} for the unlabeled G-CSF to 1610 cm^{-1} for the $^{13}C/^{15}N$-labeled protein, which can be assigned to α-helical conformation in G-CSF (Surewicz et al., 1993). For the isotope-labeled protein, the weak amide I′ band at 1677 cm^{-1} due to β-turns in G-CSF shifts to 1635 cm^{-1}. There is a distinct shoulder component at 1641 cm^{-1} for the amide I′ band of the natural G-CSF, which shifts accordingly to 1598 cm^{-1} for the $^{13}C/^{15}N$-labeled protein. These observed frequency shifts (∼40 cm^{-1}) of the amide I′ bands of G-CSF are consistent with previous reports that ^{13}C labeling of amide carbonyl (C═O) groups leads to approximately a 30−40 cm^{-1} red-shift of amide I′ band (Tadesse et al., 1991; Haris et al., 1992; Martinez et al., 1994; Zhang et al., 1994). The amide I′ band near 1640 cm^{-1} can be attributed to 3_{10} helix, as shown in a number of studies (Dwivedi et al., 1984; Holloway & Mantsch, 1989; Prestrelski et al., 1991; Miick et al., 1992). However, proteins containing β-strands and/or irregular structures may also give rise to IR bands from 1620 to 1640 cm^{-1} (Krimm & Bandekar, 1986; Susi & Byler, 1987). The crystal structure of G-CSF reveals essentially no β-strand conformation and four α-helix stretches connected by loops (Hill et al., 1993). In the connecting loop between helix A and helix B, there is a short 3_{10} helical region (from His-44 to Ser-54) which begins immediately after the first disulfide bond of G-CSF. This helical region runs almost perpendicular to the four-helical bundle and packs in front of the amino terminus of helix D. NMR data of G-CSF in solution (Werner et al.,

1994) also suggest a 3_{10} helical region involving eight residues in the same location as revealed in the crystal structure. Since the 3_{10} helix alone contains only about 5% residues of G-CSF protein, amino acids in the loop structures including AB, BC, and CD loops may also contribute significantly to the amide I′ shoulder component near 1640 cm^{-1} and to the IR intensities in the broadening feature between 1620 and 1641 cm^{-1} (Figure 2A,B). The isotopic shift of the amide I′ band of G-CSF from 1653 to 1610 cm^{-1} (Figure 2A,B) eliminates most of the spectral interference from G-CSF to the amide I′ bands of the ligand-bound receptor. The FTIR spectrum (Figure 2A, spectra C and D; Figure 2B, spectrum B) of the labeled G-CSF exhibits essentially base line IR features between 1640 and 1700 cm^{-1}, and only very weak IR intensities between 1620 and 1640 cm^{-1} due to β-turns of the labeled protein, which demonstrates the completeness of isotope labeling of G-CSF amide groups by ^{13}C and ^{15}N atoms.

Solution Conformation of the Receptor and Its Interactions with G-CSF. Figure 3 compares the original (Figure 3A) and deconvolved (Figure 3B) IR spectra of the free receptor, the unlabeled G-CSF/receptor complex, and the isotope-labeled G-CSF/receptor complex. A majority of the amide NH groups of the free receptor appear to undergo H−D exchange, as indicated by the amide II′ band centered at 1450 cm^{-1} (Figure 3A, spectrum A). However, the remaining IR intensity at 1566 cm^{-1} may also indicate the protection of some receptor amide NH groups from H−D exchange, which is common for many proteins containing mostly β-strands (Lenormant & Blout, 1953; Haris et al., 1990; Backmann et al., 1996). The lack of the FTIR spectrum of the completely exchanged receptor, however, makes it difficult to estimate the amount of amide NH groups undergoing H−D exchange for the ligand-free receptor. The spectrum of the labeled G-CSF/receptor complex (Figure 3A, spectrum C) exhibits weaker intensity in the amide II′ band at 1450 cm^{-1} than that of the free receptor (Figure 3A, spectrum A), which may indicate protection of even more receptor amide NH groups from H−D exchange within the complex than the receptor alone.

It is clear from the original IR spectra (Figure 3A, spectrum B) that the overlapping of the amide I′ bands of the unlabeled G-CSF and the receptor completely obscures the 1653 cm^{-1} band of G-CSF and makes it difficult to determine quantitatively the changes in amide I′ bands of the complex. The band overlapping cannot be resolved by either spectral deconvolution (Figure 3B, spectrum B) or the second-derivative spectrum (Figure 4, spectrum B). However, the amide I′ bands of the labeled G-CSF and the receptor are well resolved in the isotope-labeled complex (Figure 3A, spectrum C), with the amide I′ band of isotope-labeled G-CSF appearing at the low-frequency side (1610 cm^{-1}) of that of the receptor in the original IR spectrum. The two amide I′ bands of the labeled G-CSF and the receptor can be resolved by both spectral deconvolution and second-derivative calculation, as shown in Figure 3B (spectrum C) and Figure 4 (spectrum C), respectively. This separation of the two overlapping amide I′ bands immediately makes it possible to compare the amide I′ band of the receptor in the complex with that of the free receptor (Figure 3B, spectra A and C; Figure 4, spectra A and C) with little interference from the amide I′ band of G-CSF. There is no major difference between the amide I′ bands of the ligand-bound receptor and the free receptor; i.e., both exhibit intense amide I′ bands at 1636 cm^{-1} and weak intensities at 1686 cm^{-1} which are consistent with intramolecular β-strands as the dominant secondary structure. This is in agreement with the recent CD data showing that the dominant secondary structure of the G-CSF receptor is β-strand (Horan et al., 1996). However, there is a weak but significant intensity at 1652 cm^{-1} in the second-derivative spectrum (Figure 4, spectrum C) of the ligand-bound receptor whereas that of the free receptor (Figure 4, spectrum A) shows minimal intensity at the same frequency. Two possible explanations for the appearance of the weak IR band at 1652 cm^{-1} in the spectrum of the labeled G-CSF/receptor complex would be due to either some residual unlabeled G-CSF or a slight increase in α-helical content of the receptor. Since the unlabeled G-CSF gives rise to a peak IR intensity at 1653 cm^{-1}, residual unlabeled G-CSF bound to the receptor would generate a weak IR band near 1653 cm^{-1} in the spectrum of the complex. However, we think this scenario is less likely than the possibility of a real conformational change in the receptor for the following reasons. The original IR spectrum of the labeled G-CSF (Figure 2A, spectrum C) exhibits near base line IR intensity at 1653 cm^{-1}, and the deconvolved spectrum (Figure 2A, spectrum D) of the labeled G-CSF further demonstrates that there is essentially no significant IR intensity above noise level at 1653 cm^{-1}. In the second-derivative spectrum of the labeled G-CSF (Figure 2B, spectrum B), the IR band near 1653 cm^{-1} is weak and broad while the spectrum of the complex shows a sharp and discrete band near 1653 cm^{-1} (Figure 4, spectrum C). Finally, the amide I′ bands of G-CSF are only approximately one-third as intense as those of the receptor (Figure 3B, spectrum C; and Figure 4, spectrum C) because of their relative molar ratio in the complex (e.g., ∼18 kDa for G-CSF versus ∼68 kDa for the receptor considering amino acid only). As shown in the second-derivative spectrum of the complex (Figure 4, spectrum C), however, the relative intensity ratio of the amide I′ band at 1652 cm^{-1} to that of the band at 1609 cm^{-1} (I_{1652}/I_{1609}) exceeds significantly that of the labeled G-CSF alone (Figure 2B, spectrum B), which suggests that the amide I′ band at 1652 cm^{-1} in the spectrum of the labeled G-CSF/receptor complex is due to mostly the receptor rather than to residual unlabeled G-CSF. Therefore, it is likely that binding of G-CSF may induce the formation of a small amount of α-helix in the receptor. This conclusion is also consistent with the published CD data suggesting a small increase in α-helical conformation in the receptor upon binding of G-CSF (Horan et al., 1996).

To examine the structural features of G-CSF in free and complex forms, both deconvolved and second-derivative spectra of the labeled G-CSF in free form are compared with those of the labeled G-CSF in the complex (Figure 5). As shown in Figure 5A (spectra C and D), the receptor exhibits near base line IR intensity at 1598 cm^{-1} where the amide I′ band of the labeled G-CSF displays a shoulder component (Figure 5A, spectrum A). Though the presence of the weak band near 1610 cm^{-1} of the receptor increases the overall intensity of the amide I′ band of the labeled G-CSF in the complex, it should not affect the overall shape of the shoulder component at 1598 cm^{-1} because of the frequency separation. Consequently, the receptor band at 1610 cm^{-1} should have little impact on the shoulder component at 1598 cm^{-1} of the labeled G-CSF in the complex. Consistent with this notion,

additional IR data demonstrate that nonspecific interactions of G-CSF with another protein (murine tumor necrosis factor, mTNF) containing mostly β-strands and generating an IR band near 1610 cm^{-1} do not affect the shoulder component at 1598 cm^{-1} of the amide I′ band of the labeled G-CSF (data not shown). Therefore, the absence of the shoulder component at 1598 cm^{-1} in the spectra of the receptor-bound G-CSF, as shown in both deconvolved (Figure 5A, spectrum B) and second-derivative spectra (Figure 5B, spectrum B), is likely resulted from conformational changes in G-CSF rather than from any spectral interference of the receptor in the complex. As discussed under Results, the shoulder component at 1598 cm^{-1} of the amide I′ band of the labeled G-CSF is due to mostly the 3_{10} helix and the long loops connecting the four α-helices. The disappearance of this shoulder component at 1598 cm^{-1} may indicate conformational changes involving the 3_{10} helix and the surrounding loop residues of G-CSF upon complex formation. The amide I′ band of the receptor-bound G-CSF also becomes more symmetric than that of the free G-CSF (Figure 5A,B). Furthermore, the spectral features in the region 1550−1585 cm^{-1} of the two complexes containing natural and isotope-labeled G-CSF proteins are nearly identical (Figure 4, spectra B and C), which indicates that the conversion of the loops involving the 3_{10} helix to disordered structures or β-strands is unlikely. Therefore, it appears that binding of G-CSF to the receptor may lead to the loss of the 3_{10} helix in favor of α-helix, and that some adjacent loop residues near the two ends of the 3_{10} helix are most likely involved as well. The crystal structure of G-CSF reveals a number of residues before and after the 3_{10} helix not incorporated in either helix A or helix B, and these residues could be the potential candidates for the extension of α-helix in the receptor-bound G-CSF. Conformational changes in this region suggest that the AB loop region containing the 3_{10} helix may be involved in specific interactions with the receptor. The crystal structure of G-CSF shows that at the beginning of the 3_{10} helix there is a potential salt bridge between Glu-47 and His-44. The 3_{10} helical region is potentially stabilized by the interaction of these two residues. However, this salt bridge can be broken as the carboxylate group of the glutamate becomes protonated at low pH or by interacting with the receptor, which may destabilize the 3_{10} helix in favor of a regular α-helix. Interestingly, the conformational changes of G-CSF observed here share somewhat similar features with interferon-γ upon receptor binding. The crystal structure of the interferon-γ/receptor complex has revealed that the AB loop residues of interferon-γ undergo conformational change from disordered structures to 3_{10} helix upon complex formation (Walter et al., 1995).

Effects of Complex Formation on the Thermostabilities of G-CSF and Its Receptor. To determine the structural impact of complex formation on G-CSF and the receptor, we have collected FTIR spectra of G-CSF, the receptor, and the complex in the temperature range from 20 to 90 °C. As shown in Figure 6, the isotope-labeled G-CSF alone exhibits a sharp melting transition at approximately 40 °C. This thermal transition is marked by the appearences of IR bands at 1639 and 1573 cm^{-1} which are indicative of intermolecular antiparallel β-sheet, and the disappearance of the 1610 cm^{-1} band that is characteristic of α-helix (∼40 cm^{-1} red-shift compared with those of the unlabeled G-CSF; see also Figure 2). The thermal unfolding of natural G-CSF exhibits identical spectral changes to those of the labeled G-CSF except for isotopic frequency shifts (data not shown). The thermostability of the free receptor is slightly higher than that of the isolated ligand, as shown in Figure 7. The melting transition of the free receptor occurs at approximately 50 °C and is marked by the decreasing intensity of the 1636 cm^{-1} band and the increasing intensity of the 1624 cm^{-1} band. In addition, Figure 7 shows that the 1686 cm^{-1} band due to β-turns of the receptor is shifted to 1681 cm^{-1} when the receptor becomes unfolded. These changes in the amide I′ bands of the receptor are consistent with the conversion of intramolecular β-strands in native proteins to extended intermolecular β-sheets in thermally denatured proteins (Clark et al., 1981; Yang et al., 1987; Arrondo et al., 1993; Seshadri et al., 1994; van Stokkum et al., 1995).

As discussed previously, the melting transition of the G-CSF/receptor complex can be conveniently monitored by the appearances of IR bands near 1573 and 1624 cm^{-1} (Figure 8), which indicate the thermal denaturations of G-CSF and the receptor, respectively (see also Figures 6 and 7). The frequency shift of the 1686 cm^{-1} band to 1681 cm^{-1} can also be used to monitor the thermal unfolding of the receptor in the complex since the isotope-labeled G-CSF gives no spectral interference in this region (Figure 6). As shown in Figure 8, there is no significant increase in the intensity of the 1573 cm^{-1} band at temperatures up to 65 °C for G-CSF in the complex, and the median transition point appears to be in the range of 70−75 °C. In comparison to the free G-CSF (Figure 6), it is clear that thermal denaturation of G-CSF in the complex is delayed by approximately 30 °C. The α-helical conformation in G-CSF appears to be entirely stabilized by receptor binding, since the amide I′ band centered at 1609 cm^{-1} of the labeled G-CSF in the complex shows little changes in terms of intensity and bandwidth from 20 to 65 °C (Figure 8). In addition, Figure 8 shows that the thermostability of the receptor in the complex is also increased in comparison to that of the free receptor (Figure 7). Though the intensity increase of the 1624 cm^{-1} band of the complex exhibits a similar temperature profile as that of the free receptor, we believe this is due to the melting of the receptor domains which do not interact with the ligand. This proposal is supported by the following observations. First, the peak frequency of the 1636 cm^{-1} band indicative of native β-strands of the ligand-bound receptor remains unchanged even at 65 °C while for the free receptor it is nearly completely shifted to 1624 cm^{-1} at around 55 °C. This suggests that only part of the native β-structure of the ligand-bound receptor becomes unfolded at 65 °C but the ligand-free receptor unfolds entirely at this temperature. Second, the temperature profile of the 1686 cm^{-1} band of the ligand-bound receptor is markedly different from that of the ligand-free receptor. While the peak of the 1686 cm^{-1} band is completely shifted to 1681 cm^{-1} at 55 °C for the ligand-free receptor (Figure 7), it is gradually red-shifted with increasing temperature and is completely shifted to 1681 cm^{-1} at 75 °C for the ligand-bound receptor (Figure 8). This is consistent with native β-strands being more thermostable in the complex than in the free receptor.

To estimate the amount of receptor residues of which the native conformations are stabilized by G-CSF binding, we compared the deconvolved FTIR spectrum of the G-CSF/receptor complex with that of the free receptor at 55 °C

(Figure 9). The difference spectrum in Figure 9 was computed by subtracting the spectrum of the free receptor from that of the complex, and the subtraction factor was chosen so as to equalize the total integrated intensities of the positive amide I′ bands to the total integrated negative intensities in the spectral region of 1615−1700 cm^{-1}. This is a reasonable approximation considering the fact that the labeled G-CSF makes negligible spectral contributions to the amide I′ bands in the region of 1615−1700 cm^{-1} in comparison to those from the receptor. Thus, the positive amide I′ bands at 1636 and 1686 cm^{-1} in the difference spectrum are due to receptor residues with native conformations (intramolecular β-strands) in the complex while the negative amide I′ bands at 1622, 1658, 1669, and 1680 cm^{-1} are due to residues in thermally denatured states (extended intermolecular β-sheets, loops, and β-turns) in the free receptor at 55 °C. The intensity change in the amide I′ band at 1636 cm^{-1} is consistent with approximately 25% of the native β-strand conformation being potentially stabilized by the complex formation. The overall changes in the integrated intensities of the amide I′ bands at 1636 and 1686 cm^{-1} are corresponding to nearly 15% of all receptor residues. The simplest explanation for the stabilization of part of the receptor structure in the complex is by direct interactions with the ligand. This is in agreement with the results from the crystal structures of growth hormone/receptor complex and interferon-γ/receptor complex, which show that the ligand−receptor contact areas constitute roughly 10−15% of all receptor residues (de Vos et al., 1992; Clackson & Wells, 1995; Walter et al., 1995). Therefore, it seems unlikely that there are any substantial interactions between the two receptor molecules in the 2:2 complex as this would result in a greater percentage of receptor residues being stabilized than the estimation suggested by FTIR data. The current results appear to support the structural model of the G-CSF/receptor complex being similar to that of the interferon-γ/receptor complex in which the two ligand molecules lie in between the two receptor molecules (Walter et al., 1995). This model is further supported by the FTIR data (Figure 8) showing the stabilization of nearly the entire α-helical structure of G-CSF in the complex, since one side of G-CSF would be in contact with the receptor and the other side of the ligand in contact with the second G-CSF molecule in the complex. Interestingly, Figure 8 also shows that the intensity of the 1652 cm^{-1} band, indicative of the small amount of the induced α-helix present in the ligand-bound receptor, remains essentially unchanged throughout the entire temperature range, which may suggest the association of G-CSF with the receptor even at 90 °C.

In conclusion, the current data clearly demonstrate that formation of the G-CSF/receptor complex results in conformational changes in both the ligand and the receptor. In particular, the AB loop involving the unique 3_{10} helix segment in G-CSF may have specific interactions with the receptor upon complex formation. As a result of complex formation, the conformational stabilities of both G-CSF and the receptor have been greatly increased. Since G-CSF is monomeric in solution and the receptor alone has very low affinity for dimerization, it is possible that both structural changes in the ligand and the receptor could contribute to the dramatic increase in the dimeric association constant of the receptor upon binding of G-CSF (Horan et al., 1996) and consequently to the signal transduction on the cellular level.

REFERENCES

Abdel-Meguid, S. S., Shieh, H.-S., Smith, W. W., Dayringer, H. E., Violand, B. N., & Bentle, L. A. (1987) *Proc. Natl. Acad. Sci. U.S.A. 84*, 6434−6437.

Arrondo, J. L. R., Muga, A., Castresana, J., & Goni, F. M. (1993) *Prog. Biophys. Mol. Biol. 59*, 23−56.

Backmann, J., Shultz, C., Fabian, H., Hahn, U., Saenger, W., & Naumann, D. (1996) *Protein: Struct., Funct., Genet. 24*, 379−387.

Bazan, J. F. (1992) *Science 257*, 410−412.

Byler, D. M., & Susi, H. (1986) *Biopolymers 25*, 469−487.

Byler, D. M., & Susi, H. (1988) *J. Ind. Microbiol. 3*, 73.

Clackson, T., & Wells, J. A. (1995) *Science 267*, 383−386.

Clark, S. C., & Kamen, R. (1987) *Science 236*, 1229−1237.

Clark, A. H., Saunderson, D. H., & Suggett, A. (1981) *Int. J. Pept. Protein Res. 17*, 353−364.

Curless, C., Fu, K., Swank, R., Menjares, A., Fieschko, J., & Tsai, L. (1991) *Biotechnol. Bioeng. 38*, 1082−1087.

Curless, C., Baclaski, J., & Sachdev, R. (1996) *Biotechnol. Prog. 12*, 22−28.

de Vos, A. M., Ultsch, M., & Kossiakoff, A. A. (1992) *Science 255*, 306−312.

Diederichs, K., Boone, T., & Karplus, P. A. (1991) *Science 254*, 1779−1782.

Dwivedi, A. M., Krimm, S., & Malcolm, B. R. (1984) *Biopolymers 23*, 2026−2065.

Haris, P. I., & Chapman, D. (1995) *Biopolymers 37*, 251−263.

Haris, P. I., Chapman, D., Harrison, R. A., Smith, K. F., & Perkins, S. J. (1990) *Biochemistry 29*, 1377−1380.

Haris, P. I., Robillard, G. T., van Dijk, A. A., & Chapman, D. (1992) *Biochemistry 31*, 6279−6284.

Heldin, C.-H. (1995) *Cell 80*, 213−223.

Hill, C. P., Osslund, T. D., & Eisenberg, D. (1993) *Proc. Natl. Acad. Sci. U.S.A. 90*, 5167−5171.

Holloway, P., & Mantsch, H. H. (1989) *Biochemistry 28*, 931−935.

Horan, T., Wen, J., Narhi, L. O., Parker, V., & Arakawa, T. (1996) *J. Biol. Chem. Biochemistry 35*, 4886−4896.

Hubner, W., Mantsch, H. H., & Casal, H. L. (1990) *Appl. Spectrosc. 44*, 732−734.

Jackson, M., & Mantsch, H. H. (1995) *Crit. Rev. Biochem. Mol. Biol. 30*, 95−120.

Krimm, S., & Bandekar, J. (1986) *Adv. Protein Chem. 38*, 181−364.

Lenormant, H., & Blout, E. R. (1953) *Nature 172*, 770−771.

Ludlam, C. F. C., Sonar, S., Lee, C.-P., Coleman, M., Herzfeld, J., RajBhandary, U. L., & Rothschild, K. J. (1995) *Biochemistry 34*, 2−6.

Martinez, G. V., Fiori, W. R., & Millhauser, G. (1994) *Biophys. J. 66*, A65.

McKay, D. B. (1992) *Science 257*, 412−414.

Miick, S. M., Martinez, G. V., Fiori, W. R., Todd, A. P., & Millhauser, G. L. (1992) *Nature 359*, 653−655.

Mott, H. R., Driscoll, P. C., Boyd, J., Cooke, R. M., Weir, M. P., & Campbell, I. D. (1992) *Biochemistry 31*, 7741−7744.

Nagata, S., & Fukunaga, R. (1991) *Prog. Growth Factor Res. 3*, 131−141.

Nicola, N. A., Metcalf, D., Matsumoto, M., & Johnson, G. R. (1983) *J. Biol. Chem. 258*, 9017−9023.

Pandit, J., Bohm, A., Jancarik, J., Halenbeck, R., Koths, K., & Kim, S.-H. (1992) *Science 258*, 1358−1362.

Powers, R., Garrett, D. S., March, C. J., Frieden, E. A., Gronenborn, A. M., & Clore, G. M. (1992) *Science 256*, 1673−1677.

Prestrelski, S. J., Byler, D. M., & Thompson, M. P. (1991) *Int. J. Pept. Protein Res. 37*, 508−512.

Seshadri, S., Oberg, K. A., & Fink, A. L. (1994) *Biochemistry 33*, 1351−1355.

Smith, L. J., Redfield, C., Boyd, J., Lawrence, G. M. P., Edwards, R. G., Smith, R. A.G., & Dobson, C. M. (1992) *J. Mol. Biol. 224*, 899−904.

Souza, L. M., Boone, T. C., Gabriloe, J., Lai, P. H., Zaebo, K. M., Murdock, D. C., Chazin, V. R., Bruszewski, J., Lu, H., Chen,

K. K., Barendt, J., Platzer, E., Moore, M. A. S., Mertelsmann, R., & Welte, K. (1986) *Science 232*, 61−63.
Stahl, N., & Yancopoulos, G. D. (1993) *Cell 74*, 587−590.
Surewicz, W. K., Mantsch, H. H., & Chapman, D. (1993) *Biochemistry 32*, 389−394.
Susi, H., & Byler, D. M. (1987) *Arch. Biochem. Biophys. 258*, 465−469.
Tadesse, L., Nazarbaghi, R., & Walters, L. (1991) *J. Am. Chem. Soc. 113*, 7036−7037.
van Stokkum, I. H. M., Linsdell, H., Hadden, J. M., Haris, P. I., Chapman, D., & Bloemendal, M. (1995) *Biochemistry 34*, 10508−10518.
Walter, M. R., Cook, W. J., Ealick, S. E., Nagabhushan, T. L., Trotta, P. P., & Bugg, C. E. (1992) *J. Mol. Biol. 224*, 1075−1085.
Walter, M. R., Windsor, W. T., Nagabhushan, T. L., Lundell, D. J., Lunn, C. A., Zauodny, P. J., & Narula, S. K. (1995) *Nature 376*, 230−235.
Werner, J. M., Breeze, A. L., Kara, B., Rosenbrock, G., Boyd, J., Soffe, N., & Campbell, I. D. (1994) *Biochemistry 33*, 7184−7192.
Wlodawer, A., Pavlovsky, A., & Gutschina, A. (1992) *FEBS Lett. 309*, 59−64.
Yang, P. W., Matsh, H. H., Arrondo, J. L., Saint-Girons, I., Guillou, Y., Cohen, G. N., & Barzu, O. (1987) *Biochemistry 26*, 2706−2711.
Zhang, M., Fabian, H., Mantsch, H. H., & Vogel, H. J. (1994) *Biochemistry 33*, 10883−10888.

BI962713T